Münchhausen effect: tunneling in an asymmetric SQUID

A.U. Thomann*, V.B. Geshkenbein† and G. Blatter*

*Institute for Theoretical Physics, ETH Zurich, 8093 Zurich, Switzerland
†Institute for Theoretical Physics, ETH Zurich, 8093 Zurich, Switzerland
L.D. Landau Institute for Theoretical Physics, 117940 Moscow, Russia

Abstract. A classical system cannot escape out of a metastable state at zero temperature. However, a composite system made from both classical and quantum degrees of freedom may drag itself out of the metastable state by a sequential process. The sequence starts with the tunneling of the quantum component which then triggers a distortion of the trapping potential holding the classical part. Provided this distortion is large enough to turn the metastable state into an unstable one, the classical component can escape. This process reminds of the famous baron Münchhausen who told the story of rescuing himself from sinking in a swamp by pulling himself up by his own hair—we thus term this decay the 'Münchhausen effect'. We show that such a composite system can be conveniently studied and implemented in a dc-SQUID featuring asymmetric dynamical parameters. We determine the dynamical phase diagram of this system for various choices of junction parameters and system preparations.

Keywords: SQUID, Macroscopic Quantum Tunneling
PACS: 85.25.Dq, 74.50.+r

INTRODUCTION

Consider a very heavy particle ($M \to \infty$) trapped in a metastable potential minimum at temperature $T = 0$. Can it escape? The answer seems to be obvious: thermal activation is forbidden, since we are at zero temperature and tunneling is not possible either, because the particle is heavy. Matters are not that simple, however, if this heavy object is a composite one, with a quantum (light) degree of freedom coupled to the classical (heavy) one. Then the light part may tunnel out of the metastable minimum and exert a pulling force on the classical part. Once the latter is large enough to suppress the trapping barrier, the classical object is able to leave the potential well—hence a classical object may escape from a metastable state if helped by a coupled quantum degree of freedom. Two interacting particles with coordinates x_1, x_2 in 1D can be viewed as one particle in a 2D potential $V(x_1,x_2)$. Here $V(x_1,x_2)$ takes into account both the external potential and the interaction between the particles. Then the heavy and light particles map to an anisotropic mass in this problem. The Münchhausen decay corresponds to tunneling "along the light axis" and sliding thereafter along the heavy one. It is clear, that there is no problem to imagine such a 2D potential.

The above situation can be implemented experimentally in a dynamically asymmetric dc-SQUID; it is this specific realization which we will study in detail in this paper, see Fig. 1. The dynamical degrees of freedom in the dc-SQUID are the gauge-invariant phase differences φ_i, $i = 1,2$, across the two Josephson junctions. The potential energy (of a single Josephson junction) is given by $\mathscr{V}_i = E_J(1-\cos\varphi_i)$, $i = 1,2$, involving the Josephson energy $E_J = \Phi_0 I_c/2\pi c$ (with the flux unit $\Phi_0 = hc/2e$ and the critical current I_c of the junction). The kinetic energy reads $\mathscr{T}_i = (\hbar/2e)^2 C_i \dot{\varphi}_i^2/2$, where the capacitances C_i assume the role of effective masses. Hence, a SQUID featuring two Josephson junctions with equal critical current I_c but adequately chosen and strongly asymmetric capacitances, one large and one small ($C_1 \gg C_2$), effectively provides us with a classical and a quantum degree of freedom.

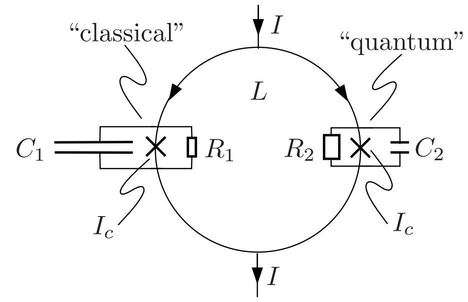

FIGURE 1. Schematics of the dynamically asymmetric dc-SQUID. Two Josephson junctions with equal critical current I_c but strongly asymmetric capacitances ($C_1 \gg C_2$) and resistances R_i are integrated in a biased (current I) superconducting loop with symmetric inductance L.

The decay process of the biased dynamically asymmetric SQUID proceeds in the following manner: The bias I, leading to a term $\propto -I(\varphi_1+\varphi_2)$ in the potential, turns a stable state of the washboard potential into a metastable one. As junction 1 features a large capacitance, we assume its dynamics to be strictly classical. If the bias I is large enough, a (imaginary time) decay process involving only the quantum junction (at constant φ_1) is enabled. This phase slip leads to the entry of magnetic flux into the ring. Given the inductive coupling $\propto 1/L$ (inductance L), the current through the classical junction is enhanced and it may eventually become overcritical, thus decaying via a classical real time trajectory.

SETUP

We start from the capacitively shunted junction model (CSJ), where the dc-SQUID, biased with a current I, is described by the Lagrangian

$$\mathscr{L} = \sum_{i=1}^{2} \left[\left(\frac{\Phi_0}{2\pi c} \right)^2 \frac{C_i}{2} \dot{\varphi}_i^2 - E_J (1 - \cos \varphi_i) \right] + \frac{\Phi_0 I}{2\pi c} \frac{\varphi_1 + \varphi_2}{2} - \left(\frac{\Phi_0}{2\pi c} \right)^2 \frac{(\varphi_1 - \varphi_2)^2}{2L}; \quad (1)$$

here, we have assumed that the inductance L of the SQUID is symmetrically distributed. The Lagrangian $\mathscr{L}$ generates the equations of motion

$$m_i \ddot{\varphi}_i + \eta_i \dot{\varphi}_i = -\partial_{\varphi_i} v(\varphi_1, \varphi_2), \quad (2)$$

with the 'masses' $m_i = \Phi_0 C_i / 2\pi c I_c$ and where we have added the dissipative terms $\eta_i \dot{\varphi}_i$ with the damping parameters $\eta_i = \Phi_0 / 2\pi c I_c R_i \propto 1/R_i$, R_i the normal resistances of the junctions; the potential (illustrated in Fig. 2) is given by

$$v(\varphi_1, \varphi_2) = 2 - \cos \varphi_1 - \cos \varphi_2 - j(\varphi_1 + \varphi_2) + \frac{k}{2} (\varphi_1 - \varphi_2)^2, \quad (3)$$

with the dimensionless current $j = I/2I_c$, the coupling constant $k = \Phi_0 / 2\pi c I_c L$ and where energies are measured in units of E_J.

Residing in a symmetric ($\varphi_1 = \varphi_2 = \arcsin i$) metastable state of the potential $v(\varphi_1, \varphi_2)$ at finite bias current i, the classical version of the system described through Eq. (2) cannot decay at zero temperature. Here, we are investigating the case where junction one, featuring a large capacitance C_1, is assumed to behave strictly classical, whereas the dynamics of junction 2 is characterized by large quantum fluctuations. This can be achieved through a suitable choice of parameters, i.e., a small capacitance C_2, while keeping $E_J \gtrsim E_{C2} = e^2/2C_2$ such that we remain in a quasi-classical regime.

In the system under consideration, different scenarios can arise depending on the strength of the dissipation as quantified by the dimensionless damping parameter

$$\alpha_i = (2 R_i C_i \omega_{pi})^{-1}, \ i = 1, 2, \quad (4)$$

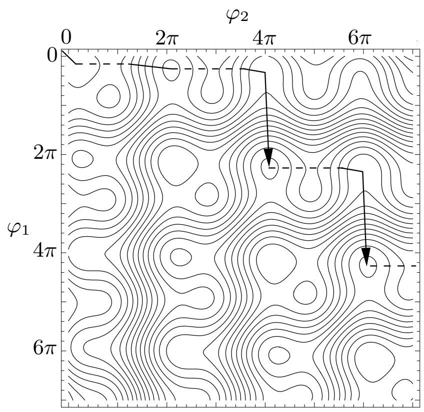

FIGURE 2. Illustration of the decay sequence of the dynamically asymmetric SQUID ($j = 0.5$, $k = 0.04$). The initial metastable well is unstable w.r.t. the macroscopic quantum tunneling of the small junction 2. A continuous sequence of phase slips takes the system to a state which is classically unstable. In the following, the (classical) relaxation of the large junction 1 and the quantum decay of junction 2 alternate and lead to a finite voltage state of the SQUID.

where, at $j = 0$, the plasma frequency $\hbar\omega_{pj} = (8 E_J E_{Ci})^{1/2}$. The simplest case is the overdamped situation $\alpha_1, \alpha_2 > 1$, where the dynamics of the classical junction is viscous and both relaxation and tunneling of the quantum junction are incoherent [2, 1]. We will analyze this situation in detail in the next section; the obtained results are also relevant for other choices of parameters, c.f. below.

PHASE DIAGRAM - STRONG DAMPING

In the following, we determine for which currents i and coupling constants k a zero temperature decay of a symmetric metastable state ($\varphi_1 = \varphi_2 = \arcsin i$, up to an arbitrary multiple of 2π) is allowed in the interferometer potential $v(\varphi_1, \varphi_2)$. The result is displayed in a dynamical phase diagram in the j-k-plane, see Fig. 4, where the critical line $j_c(k)$ separates regions where this decay is prohibited (localized state) from regions where it is allowed (delocalized).

Assuming junction 1 to behave strictly classical, (i.e. considering the limit of very large C_1), a quantum decay of the SQUID in a metastable state can only occur at fixed φ_1, i.e. through an imaginary-time trajectory of φ_2 in the effective potential $v_{\text{eff}}(\varphi_2) = v(\varphi_1 = \text{const.}, \varphi_2)$, see Fig. 3. We will adopt this approximation for all tunneling processes throughout the discussion. For sufficiently large j, the quantum degree of freedom φ_2 undergoes tunneling to a new local minimum nearby $2\pi n$, while the classical degree of freedom $\varphi_1 = \arcsin j$ remains localized, thus allowing a flux $\simeq n\Phi_0$, $n \in \mathbb{N}$ to

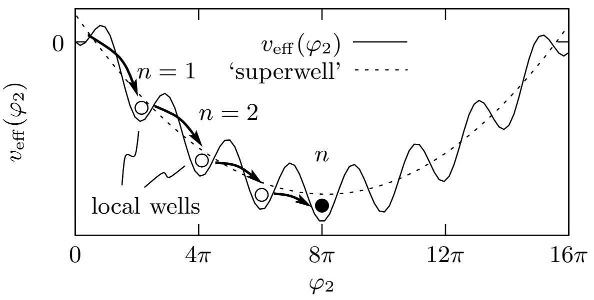

FIGURE 3. Effective potential $v_{\rm eff}(\varphi_2) = v(\varphi_1 = \text{const.}, \varphi_2)$ (solid line) and the parabola remaining after dropping $\cos\varphi_2$ (dashed line) for $j = 0.5$, $k = 0.02$ and $\varphi_1 = \arcsin j$. The bullets and arrows illustrate the sequential decay of the quantum phase φ_2 to the ground state for the case of strong damping.

enter the SQUID loop, cf. Fig. 3. If the resulting force on the classical phase φ_1 is sufficiently large, the Münchhausen decay is enabled with a classical decay of φ_1 and successive iteration of quantum decay (directed along φ_2, flux entry) and classical relaxation (directed mainly along φ_1, flux exit), cf. Fig. 2.

For undercritical currents $j < 1$ the described initial state, $\varphi_1 = \varphi_2 = \arcsin j$, is stable against a decay involving the classical junction; however it is, for $k < j/(\pi - \arcsin j)$, unstable with respect to a quantum decay of φ_2 since the minimum of $v_{\rm eff}(\varphi_2)$ near $\varphi_2 \approx 2\pi$ is lowered below the initial one and one or more phase slips of φ_2 are possible. In order to determine whether the SQUID will remain in a stable or enter a finite voltage state at given j,k we proceed in two steps: First, we have to determine where the successive quantum tunneling of φ_2 comes to a halt, i.e., which side minimum is quantum-stable. This is equivalent to finding the global minimum of the effective potential $v_{\rm eff}(\varphi_2)$. Fixing the phase across the classical junction $\varphi_1 = \arcsin j$, one immediately sees that the quantum-stable minimum is the one near $\varphi_2 \approx 2\pi n$ if n is the largest integer, such that

$$k < k^+_{c,n}(j) \approx \frac{j}{(2n-1)\pi - \arcsin j}. \tag{5}$$

The sequence of phase slips of the quantum junction leads to an accumulation of magnetic flux in the SQUID loop, inducing a screening current. Consequently, the current through junction 2 is reduced whilst that through junction 1 is increased. The magnitude of the induced current depends strongly on the coupling constant k; for given n, it is only large enough to drive the classical junction overcritical if

$$k > k^-_{c,n}(j) \approx \frac{1-j}{(2n-1/2)\pi + \arcsin(2j-1)}. \tag{6}$$

If this is the case, the SQUID enters a finite voltage state where quantum tunneling of junction 2 (an approximate flux unit enters the loop) and classical relaxation of junction 1 (flux leaves the loop) interchange sequentially (see Fig. 2). If $k < k^-_{c,n}(j)$, the SQUID resides in a localized state and a further increase in j is necessary to drive the system unstable. The two conditions Eqs. (5) and (6) generate a web of crossing lines in the j,k-plane ($j^+_{c,n}(k)$ and $j^-_{c,n}(k)$ are inversed expression to Eqs. (5) and (6) correspondingly), determining the critical line $j_c(k)$ marking the dynamic transition from a localized to a delocalized state (Fig. 4). In the limit $k \to 0$, where the cosine in the potential Eq. (3) becomes a small correction to the parabola, the critical line $j_c(k)$ approaches 1/2; this indicates that all current is redirected through junction 1 and delocalization takes place at $I = I_c$, the critical current of a single junction,

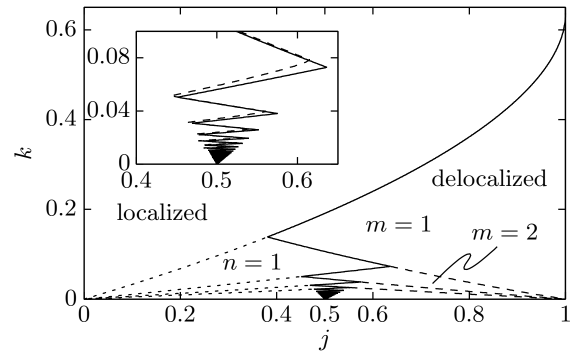

FIGURE 4. Phase diagram of the dynamically asymmetric dc-SQUID as a function of bias current $j = I/2I_c$ and inductive coupling $k = \Phi_0 c/2\pi L I_c$. Here, we assume strong damping $\alpha_{p,1} \gg 1$ and $\alpha_{p,2} > 1$. The effective critical current $j_c(k)$ (solid line) marks the boundary between a localized classical junction (lower bias $j < j_c$) and a delocalized classical junction ($j > j_c$), corresponding to a finite voltage state of the SQUID. Branches with negative slope are determined by a classical instability (mainly along φ_1), while those with positive slope are determined by a quantum instability of the light junction. For $j < j_c(k)$, the dotted lines $j^+_{c,n}(k)$ mark the entry of flux through the quantum junction (the integer n approximately quantifies the flux through the ring in the stable state); these lines can be measured via monitoring of the flux threading the loop. For $j > j_c(k)$, the dashed lines $j^-_{c,m}(k)$ mark the minimum number m of flux units necessary to delocalize the classical junction. The inset shows a comparison between the approximate result (solid line) and the exact numerical result (dashed).

The simple arguments above have to be refined in order to obtain the precise location of the critical line $j_c(k)$. First, the condition of classical stability is but the standard determination of the critical current of a dc-SQUID's asymmetric minimum [3]. In our case, where classical stability along the φ_2-direction is guaranteed, the relevant set of equations is given by

$$\sin(\bar{\varphi}_1^n) = j - k_{c,n}(\bar{\varphi}_1^n - \bar{\varphi}_2^n), \tag{7}$$

$$\sin(\bar{\varphi}_2^n) = j + k_{c,n}(\bar{\varphi}_1^n - \bar{\varphi}_2^n), \tag{8}$$

$$\cos\bar{\varphi}_1^n \cos\bar{\varphi}_2^n = -k_{c,n}(\cos\bar{\varphi}_1^n + \cos\bar{\varphi}_2^n), \tag{9}$$

and has to be solved (numerically) for $k_{c,n}(j)$ and $\bar{\varphi}_{1,2}^n$, the coordinates of the true minima near $\varphi_1 = \arcsin j$, $\varphi_2 = 2\pi n$. Eq. (6) is an approximate solution to Eqs. (7)-(9) in the limit of $k \ll 1$. Second, as tunneling of the quantum junction might be enabled only after the relaxation of the classical junction to a minimum, condition Eq. (5) has to be corrected to

$$k_{c,n}^{+}(j) = \frac{j}{(2n-1)\pi - \bar{\varphi}_1^{n-1}}, \tag{10}$$

taking into account the change of the effective potential $v_{\mathrm{eff}}(\varphi_2)$ upon a change in φ_1. The exact numerical solutions of Eqs. (7)-(9) and (10) are shown in the inset of Fig. 4, where the approximate solution is seen to be rather precise.

The critical current line $j_c(k)$ is constructed from interchanging segments of $j_{c,n}^{+}(k)$ and $j_{c,n}^{-}(k)$, resulting in the dynamical phase diagram, Fig. 4. Note that the different nature of the decay, classical or quantum, associated with the two types of critical lines may allow for an experimental distinction: Ramping the current past a $^{+}$-type segment of $j_c(k)$ triggers a *quantum* decay with a broad histogram describing multiple measurements. A $^{-}$-type segment of $j_c(k)$ triggers a *classical* decay with a sharp histogram (the quantum decay of φ_2 needs to have occurred already, which limits the ramping speed before reaching the critical line). Note that the lines $j_{c,n}^{+}(k)$ are detectable throughout all the stable portion of the phase diagram, e.g., via a measurement of the flux threading the loop (the flux increases by approximately one flux unit upon crossing the dotted lines in Fig. 4).

WEAK DAMPING

The behavior of the system for weak damping $\alpha_{LC,2} \ll 1$, $\alpha_{p,i} \ll 1$ strongly depends on preparation. Here we are not going to discuss all the possible situations. Instead, we concentrate on the most interesting case. Depending on parameters, after tunneling the quantum degree of freedom may become delocalized between different local wells of the 'super-well' Fig. 3 . These side-well states have different lifetimes. The dissipation described by the normal resistance R in the RCSJ-equation of motion, cf. Eq. (2), leads to typical finite lifetimes $\tau_2 \sim RC_2 = 1/2\alpha_2\omega_{p,2}$ of the excited states $|l\rangle$ of the quantum junction.[4] A much longer lifetime $\tilde{\tau}_2$ shows up if the quantum junction is trapped in a local ground state of a side-well in $v_{\mathrm{eff}}(\varphi_2)$, cf. Fig. 5. The decay then is protected through a large barrier E_b, enhancing the typical lifetime to a value $\tilde{\tau}_2$, with $\tau_2 \ll \tilde{\tau}_2 \propto \exp(2\gamma\sqrt{E_J/4E_{c,2}})$.[5] Thus, there are two (extreme) ways how a highly exited state in the 'super-well' of $v_{\mathrm{eff}}(\varphi_2)$ can decay, see Fig. 5, either via states within the super-well involving the typical lifetime τ_2, or via states involving a tunneling process, resulting in an exponentially larger decay time of the order of $\tilde{\tau}_2$.

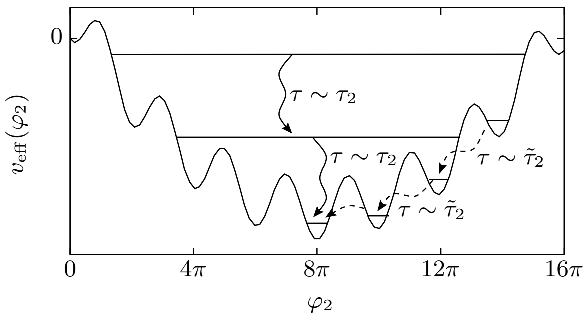

FIGURE 5. Illustration of decay sequences of an excited 'super-well'-state of the quantum junction in the effective potential $v_{\mathrm{eff}}(\varphi_2)$. Solid arrows indicate a decay sequence involving only states within the 'super-well' with a typical decay time τ_2. The dashed arrows illustrate another (extreme) decay sequence, involving localized states in the side-minima of $v_{\mathrm{eff}}(\varphi_2)$. The decay time then involves the typical lifetime $\tilde{\tau}_2 \gg \tau_2$ of local ground states within side-wells.

The quantum junction may be trapped in any side-well for a significant amount of time. If it gets trapped in a distant side-well (large values of φ_2 in Fig. 5) it exerts a larger force on the classical junction. The classical junction is pulled out of its metastable state more efficiently in this case. We can define two extreme values for the critical current, a lower limit $j_c^{(1)}(k)$ arising from the largest attainable fluxon index n, and an upper limit $j_c^{(2)}(k)$ associated with the index n of the global minimum of the quantum junction. The resulting phase diagram is displayed in Fig. 6.

The two critical lines $j_c^{(1)}(k)$ and $j_c^{(2)}(k)$ define a broad intermediate regime, see the grey area in Fig. 6, where the decay of the system is of probabilistic nature. The system is localized for $j < j_c^{(1)}(k)$ and delocalized for $j > j_c^{(2)}(k)$. The decay probability in the intermediate regime is neither 0 nor 1, but depends on which minimum the quantum junction φ_2 decays to.

EXPERIMENTAL IMPLEMENTATION

The running state following a Münchhausen decay is associated with a finite time-averaged voltage across the device. The above results thus can be tested experimentally by measuring the voltage drop as a function of the

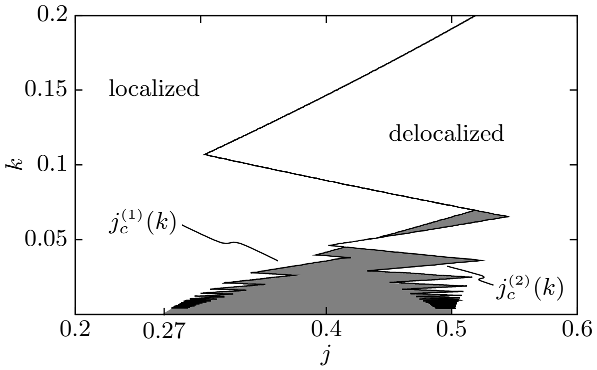

FIGURE 6. Effective critical currents of the dynamically asymmetric SQUID for $\tilde{\tau}_2 \gg \omega_{p1}^{-1}$ and fast ramping. The system always turns resistive for $j > j_c^{(2)}(k)$ but never turns resistive for $j < j_c^{(1)}(k)$. For $j_c^{(1)} < j < j_c^{(2)}$ the delocalization of the system is determined by the statistical nature of the decay process of the quantum junction involving the side minima.

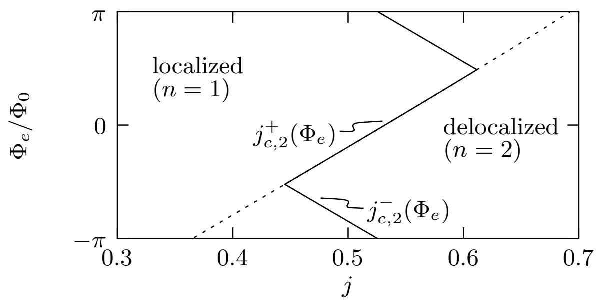

FIGURE 7. Phase diagram of the dynamically asymmetric SQUID in the strong damping case as a function of the externally applied flux Φ_e and bias current j. Here, the coupling $k \propto L^{-1}$ is fixed at a value $k = 0.06$; the critical lines in the diagram correspond to $n = 2$. The critical line is periodic in Φ_e with a period Φ_0, a consequence of the invariance under the replacements $\Phi_e/\Phi_0 \to \Phi_e/\Phi_0 \pm 1$ and $n \to (n \pm 1)$.

applied bias current I and of the inductance L of the SQUID.

Mapping any part of $j_c(k)$ requires changing the coupling $k \propto L^{-1}$. It is difficult to vary the induction of the loop, which is usually fixed after fabrication. One (although rather difficult) way to modify it is to install a diamagnetic shield. Another way to trace the critical current line is obtained by applying an external magnetic flux Φ_e to the sample, in which case the potential Eq. (3) has to be replaced by

$$\begin{aligned} v(\varphi_1, \varphi_2) &= 1 - \cos\varphi_1 + 1 - \cos\varphi_2 \\ &\quad - j(\varphi_1 + \varphi_2) + \frac{k}{2}(\varphi_1 - \varphi_2 - 2\pi\Phi_e/\Phi_0)^2. \end{aligned} \quad (11)$$

The critical current j_c then can be studied as a function of Φ_e. The analysis proceeds in the same way as before: a change in k altering the opening angle of the parabola in $v(\varphi_1, \varphi_2)$ is replaced by a shift in the parabola's position due to the applied flux Φ_e.

The results are invariant under the shifts $\Phi_e/\Phi_0 \to \Phi_e/\Phi_0 \pm 1$ and $n \to (n \pm 1)$. The Münchhausen decay thus can be studied within a finite interval, e.g. $\Phi_e/\Phi_0 \in [-0.5, 0.5]$, and the resulting phase diagram is displayed in Fig. 7.

Biasing the SQUID with an external magnetic flux has a convenient side effect: For negative flux Φ_e, the crossing point of $j^+_{c,n}(k)$ and $j^-_{c,n}(k)$ is shifted to larger values of k and the tunneling barrier for φ_2 is lowered, allowing to study the Münchhausen effect using a SQUID with considerably smaller inductance and hence smaller size.

CONCLUSION

We have shown that a system consisting of two degrees of freedom can escape out of a metastable state, even if one of the degrees behaves *fully* classical, provided the second one shows quantum behavior. This can be realized in a dynamically asymmetric dc-SQUID. The "Münchhausen-decay" involves tunneling of the quantum junction, where magnetic flux accumulates in the superconducting ring and eventually redirects enough current through the classical junction as to drive it overcritical. The resulting phase diagram of the SQUID appears to be unexpectedly rich.

ACKNOWLEDGMENTS

We thank A. Larkin, A. Ustinov, G. Lesovik, A. Lebedev, A. Wallraff, and E. Zeldov for interesting discussions and acknowledge support of the Fonds National Suisse through MaNEP.

REFERENCES

1. A.O. Caldeira and A.J. Leggett, *Ann. Phys. (NY)* **149**, 374 (1983).
2. A.J. Leggett, S. Chakravarty, A.T. Dorsey, M.P.A. Fisher, A. Garg, and W. Zwerger, *Rev. Mod. Phys.* **59**, 1 (1987).
3. W.-T. Tsang and T.V. Duzer, *J. Appl. Phys.* **46**, 4573 (1975).
4. D. Esteve, M.H. Devoret, and J.M. Martinis, *Phys. Rev. B* **34**, 158 (1986).
5. D.V. Averin, J.R. Friedman, and J.E. Lukens, *Phys. Rev. B* **62**, 11802 (2000).